

# Regenerative capacity of adult cortical thymic epithelial cells

Immanuel Rode<sup>1</sup> and Thomas Boehm<sup>2</sup>

Department of Developmental Immunology, Max Planck Institute of Immunobiology and Epigenetics, D-79108 Freiburg, Germany

Edited by Max D. Cooper, Emory University, Atlanta, GA, and approved January 23, 2012 (received for review November 16, 2011)

**Involvement of the thymus is accompanied by a decline in the number of thymic epithelial cells (TECs) and a severely restricted peripheral repertoire of T-cell specificities. TECs are essential for T-cell differentiation; they originate from a bipotent progenitor that gives rise to cells of cortical (cTEC) and medullary (mTEC) phenotypes, via compartment-specific progenitors. Upon acute selective near-total ablation during embryogenesis, regeneration of TECs fails, suggesting that losses from the pool of TEC progenitors are not compensated. However, it is unclear whether this is also true for the compartment-specific progenitors. The decline of cTECs is a prominent feature of thymic involution. Because cTECs support early stages of T-cell development and hence determine the overall lymphopoietic capacity of the thymus, it is possible that the lack of sustained regenerative capacity of cTEC progenitor cells underlies the process of thymic involution. Here, we examine this hypothesis by cell-type-specific conditional ablation of cTECs. Expression of the human diphtheria toxin receptor (hDTR) gene under the regulatory influence of the chemokine receptor *Cxcr1* gene renders cTECs sensitive to the cytotoxic effects of diphtheria toxin (DT). As expected, DT treatment of preadolescent and adult mice led to a dramatic loss of cTECs, accompanied by a rapid demise of immature thymocytes. Unexpectedly, however, the cTEC compartment regenerated after cessation of treatment, accompanied by the restoration of T-cell development. These findings provide the basis for the development of targeted interventions unlocking the latent regenerative potential of cTECs to counter thymic involution.**

thymopoiesis | transgenesis

**T**-cell production in the thymus declines with age, leading to a severely restricted peripheral repertoire of T-cell specificities (1). All strategies, including gonadectomy, to overcome the deleterious effects of thymic involution merely result in a transient increase in thymus size but do not prevent its eventual decline (2–6). These observations suggest that age-related decline is an intrinsic property of thymopoiesis. Thymic involution is accompanied by a decline in the number of thymic epithelial cells (TECs) (7) that constitute the major thymopoietic stromal component. TECs originate from a bipotent progenitor that gives rise to cells of cortical (cTEC) and medullary (mTEC) phenotypes (8, 9), and are essential for the attraction and specification of T-cell progenitors and their subsequent selection (10, 11). It appears that the pool of TEC progenitors is established during embryogenesis and, due to limited niche space, comprises a fixed number of such cells (12); in addition, the depletion of TECs during early embryogenesis is not compensated during later stages of development (13), suggesting that the bipotent TEC progenitor lacks appreciable self-renewing properties. Whether the same is also true for compartment-specific progenitors (9, 14) (those giving rise to cTECs and mTECs) is, however, unknown. Several mechanisms could explain the decline in TEC numbers that occurs during aging. For instance, it is possible that the postnatal thymus fails to provide signals that stimulate epithelial progenitor cells to self-renew; alternatively, transit amplification of progenitors en route to the terminally differentiated epithelium might be compromised.

Epithelial cells in the thymic cortex (cTECs) support the early stages of T-cell development (10, 11, 15); hence, the number of cTECs determines the overall lymphopoietic capacity of the thymus (8, 9, 12). Because the number of cTECs begins to decline in adolescence (7), it is possible that the lack of sustained regenerative capacity of cTEC progenitor cells contributes to the process of thymic involution. To examine the regenerative potential of cTECs, we established a transgenic cTEC-specific cell ablation procedure that revealed an unexpected and sustained capacity of compensatory growth after acute ablation.

## Results

**Selective Ablation of cTECs.** So far, it has proved impossible to achieve cell-type-specific genetic manipulation of cTECs, primarily due to the lack of suitable transcriptional regulatory sequences specifically addressing the cTEC compartment. To establish such a system, we focused our attention on the chemokine receptor *Cxcr1* gene (16). Using a bacterial artificial chromosome encompassing the *Cxcr1* gene as template, we inserted the human diphtheria toxin (DT) receptor (*DTR*) gene into the coding exon of this gene (Fig. 1A). Subsequent analyses were carried out in *Cxcr1<sup>eGFP/+</sup>;Cxcr1:DTR* mice carrying a wild-type allele of *Cxcr1*, an *eGFP* knock-in on the second allele of the *Cxcr1* locus (16), and additionally the BAC-derived human *DTR* transgene. Relevant stromal populations were isolated using a multi-step flow sorting protocol (17) (Fig. 1B) and the expression levels of the three forms of *Cxcr1* genes were analyzed by RT-qPCR (Fig. 1C). The results indicate that expression in cTECs far exceeds that in other stromal cell types. To examine whether expression of *DTR* could be harnessed to achieve cTEC-specific toxicity, 1-wk-old mice were injected with DT and the absolute numbers of stromal cells were determined 24 h later. The number of cTECs in treated mice was found to be drastically reduced, whereas the numbers of mesenchymal cells, endothelial cells, and medullary thymic epithelial cells were not affected (Fig. 1D and E). Additional experiments validated cTEC as the sole target of DT-mediated cytotoxicity. When thymic lobes of newborn mice were transplanted under the kidney capsule of nontransgenic syngenic recipients and treated with DT, the number of thymocytes [particularly CD4<sup>+</sup>CD8<sup>+</sup> double-positive (DP) cells] was greatly diminished only in the transplanted transgenic lobes; cellularity remained unchanged in the wild-type transplants and also in the endogenous thymi of recipients of both types of transplants, ruling out systemic effects (Fig. S1). Whereas this observation suggests that DT acts on the stromal compartment in the thymus, the possibility had to be excluded that hematopoietic cells ectopically

Author contributions: I.R. and T.B. designed research; I.R. performed research; I.R. and T.B. analyzed data; and I.R. and T.B. wrote the paper.

The authors declare no conflict of interest.

This article is a PNAS Direct Submission.

<sup>1</sup>Present address: Division of Cellular Immunology, German Cancer Research Center, D-69120 Heidelberg, Germany.

<sup>2</sup>To whom correspondence should be addressed. E-mail: boehm@immunbio.mpg.de.

This article contains supporting information online at [www.pnas.org/lookup/suppl/doi:10.1073/pnas.1118823109/-DCSupplemental](http://www.pnas.org/lookup/suppl/doi:10.1073/pnas.1118823109/-DCSupplemental).

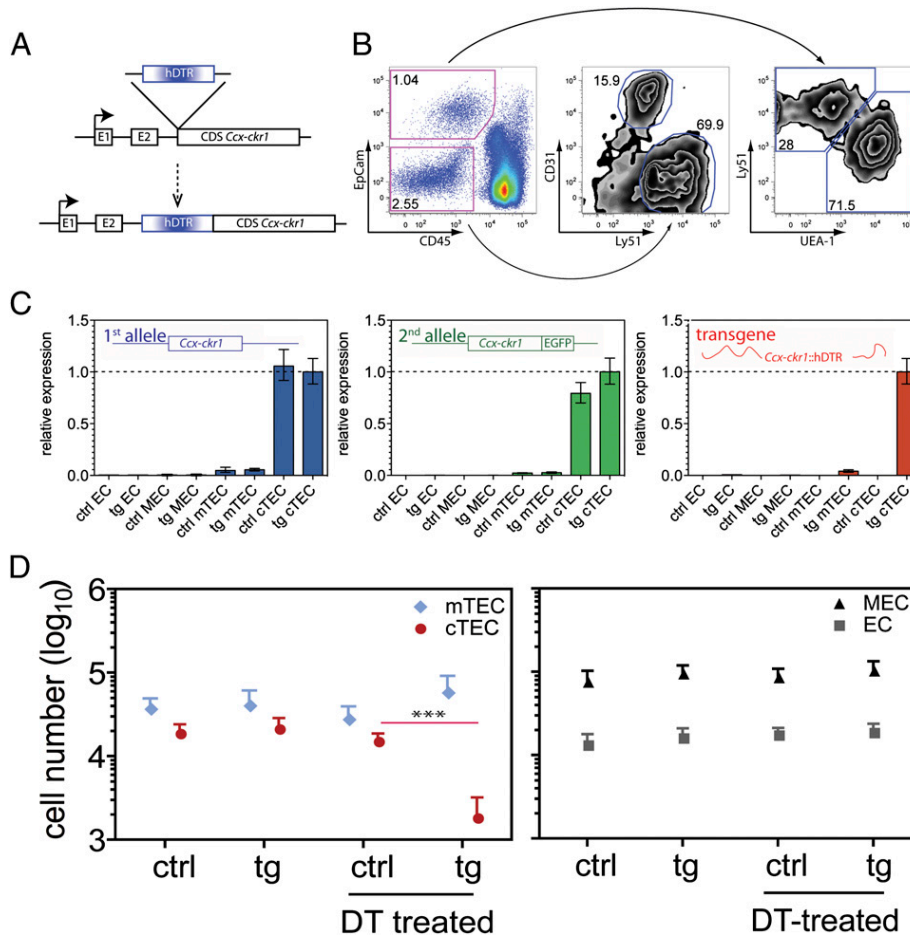


**Fig. 1.** cTEC specific cytoablation. (A) Schematic representation of the *Ccx-ckr1*:DTR transgene. (B) Flow cytometric isolation of stromal components. Neural-crest derived mesenchymal cells (MEC), EpCam<sup>-</sup>, CD45<sup>-</sup>, CD31<sup>-</sup>, Ly51<sup>+</sup> marker (Center); endothelial cells (EC), EpCam<sup>-</sup>CD45<sup>-</sup>CD31<sup>+</sup>Ly51<sup>-</sup> (Center); cTECs, EpCam<sup>+</sup>CD45<sup>-</sup>Ly51<sup>+</sup>UEA-1<sup>-</sup> (Right); and mTECs, EpCam<sup>+</sup>CD45<sup>-</sup>Ly51<sup>-</sup>UEA-1<sup>+</sup> (Right). (C) Expression levels of the endogenous *Ccx-ckr1* gene, the *Ccx-ckr1*:eGFP knock-in allele, and the *Ccx-ckr1*:hDTR transgene in *Ccx-ckr1*<sup>eGFP/+</sup> control (ctrl) and *Ccx-ckr1*<sup>eGFP/+</sup>; *Ccx-ckr1*:DTR transgenic (tg) mice. Results of quantitative RT-PCR normalized to the expression levels of *Hprt* are expressed relative to the levels of *Ccx-ckr1*:hDTR transgenic cTECs (dashed line). (D) Absolute numbers of TEC subsets (Left) and MECs and ECs (Right) of untreated and diphtheria toxin (DT)-treated nontransgenic (ctrl) or hDTR-transgenic mice (tg); animals received a single injection of DT (30 ng/g body weight, i.p.) and were analyzed 1 d (P8) thereafter. Statistical analysis was performed using Fisher's *t* test (\*\*\*) *P* < 0.001.

express the *Ccr-ckr*:DTR transgene. Thymocytes originating from the bone marrow of wild-type and transgenic donor cells were resistant to DT, confirming the stroma-specific effect of the *Ccx-ckr*:DTR transgene (Fig. S2). Collectively, these results establish that the regulatory elements of the *Ccr-ckr1* gene enable the specific expression of transgenes in cTECs.

**Structure of Cortical Microenvironment After Acute Ablation.** We examined the composition of the cortical microenvironment by immunohistochemistry after cTEC ablation; this examination revealed that only few and small clusters of cytokeratin 8-positive cTECs remained in the thymus of *Ccx-ckr1*:hDTR transgenic mice 24 h after DT treatment (Fig. 2A). Whereas the cortical epithelium was severely diminished, the mesenchymal network in the cortex remained intact (Fig. 2B). The acute collapse of the cortical stroma led to a reduction in immature thymocytes, which are typically located within the cortical environment (10, 15, 16). When analyzed 3 d after treatment (postnatal day 10, P10), immature double-negative stage 2 and 3 thymocytes (DN2–3) were essentially absent (Fig. 2C). One week after treatment (P14), the same was observed for CD4<sup>+</sup>CD8<sup>+</sup> double-positive (DP) cells (Fig. 2D). By contrast, CD4 and CD8 single-positive (SP) cells located in the medulla were only mildly affected (Fig. 2E and F).

However, the reduction of SPs is likely to be an indirect effect, as the supply of immature progenitors is acutely interrupted. The loss of cTECs not only disturbs the environment required for the attraction and settling of early thymocyte progenitors (present in the double-negative compartment), leading to a reduction of cells destined to become double-positive thymocytes, it also affects the pool of immature double-positive thymocytes that are destined to differentiate into single-positive thymocytes. The known sequence of thymocyte differentiation is mirrored by the consecutive loss of DN2–3, DP, and SP thymocytes after cTEC ablation observed here. Collectively, these experiments indicate that acute loss of cTECs is accompanied by a dramatic reduction in immature thymocyte populations, providing direct evidence that the presence of the cortical epithelium is required for the maintenance of early T-cell subsets in the thymus.

**Recovery of cTECs.** We investigated whether the cTEC compartment could recover from near-total ablation at P7. Although flow cytometry reveals virtually no CD45<sup>-</sup>EpCam<sup>+</sup>UEA-1<sup>-</sup>Ly51<sup>+</sup> cTECs at P8 in DT-treated animals, these cells reappeared shortly thereafter and, at P14, already constituted a sizeable fraction of thymic epithelial cells (Fig. 3A). This restoration of the cortical microenvironment was also evident

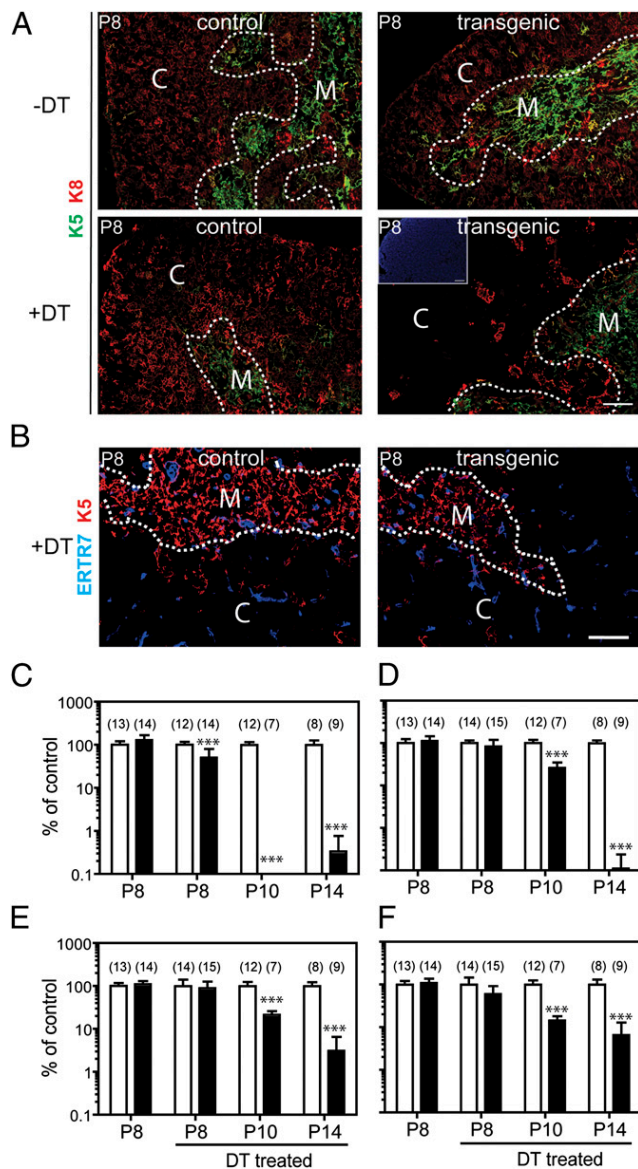


**Fig. 2.** Loss of cTECs abrogates T-cell differentiation. (A) Representative cryosections of thymic tissue from mice treated as in Fig. 1D. Sections were stained with antibodies for an mTEC marker (cytokeratin 5, K5, green fluorescence) and a cTEC marker (cytokeratin 8, K8, red fluorescence). At this point the thymic cortex still contains many lymphocytes (*Inset*), as revealed by intense nuclear DNA staining (DAPI, blue fluorescence). (Scale bar, 100  $\mu$ m.) (B) Representative cryosections as in A stained with antibodies for mesenchymal cells (ERTR7, blue fluorescence) and K5. (Scale bar, 100  $\mu$ m.) Other designations in A and B as in legend to Fig. 1. (C–F) Differential effect on thymocytes 1, 3, and 7 d after DT treatment. (C) DN2–3 ( $Lin^{-}CD25^{+}$ ). (D) DP thymocytes ( $CD4^{+}CD8^{+}$ ). (E)  $CD4^{+}$  single positive. (F)  $CD8^{+}$  single positive. Cell numbers are expressed relative to control mice (mean  $\pm$  SD) (for absolute numbers see [Dataset S1](#)); the number of animals in each group is given in parentheses *Above* bars. Statistical analysis was performed using Fisher's *t* test ( $***P < 0.001$ ).

from immunohistological examinations (Fig. 3B). The observed regenerative capacity of the cortical compartment is compatible with the presence of progenitors for cTECs at both embryonic and postnatal stages (8, 9, 18). A detailed analysis of the hematopoietic compartment in recovered thymi indicated that the reappearance of cTECs was accompanied by a near-complete restoration of DN and DP thymocyte numbers (Fig. 3C; for

absolute cell numbers see [Dataset S1](#)). Notably, the numbers of DN2–3 cells decreased more rapidly and recovered earlier than those of DP cells (Figs. 2 C–F and 3C); this time course is compatible with the known developmental sequence of thymocytes in which DN precede DP cells. At P31 (i.e., 24 d after toxin treatment), the DP compartment had recovered to 22% and the DN2–3 compartment to  $\sim$ 36% of age-matched control levels. Of note, these values underestimated the regenerative potential because of the significant growth of the thymus in control animals during the first month after birth ([Dataset S1](#)). Collectively, these results provide compelling evidence that cTEC recovery is the decisive factor in thymocyte recovery.

**Regeneration of cTECs in Adult Mice.** We examined the regenerative capacity of the cortical compartment in *Ccx-ckr1:hDTR* transgenic mice that had been treated with a single dose of DT at 2–3 mo of age. In contrast to the recovery of thymopoietic activity observed in all mice treated at P7 (Fig. 3A–C), thymopoietic activity in adult mice was restored only in females (Fig. 4A) and not in males (Fig. 4B). Irrespective of this sexually dimorphic response, these results demonstrate that the cTEC compartment is capable of substantial regenerative growth and that this capacity remains latent during physiological thymic involution. Next, we examined whether regeneration was sensitive to androgens, because surgical or pharmacologically induced castration of adult male mice has been shown to lead to a transient increase in the number of thymocytes (2, 3, 5). We observed that castration of male *Ccx-ckr1:hDTR* transgenic mice after DT treatment has a similar effect (Fig. 4C), compatible with the finding that cortical epithelial cells express the androgen receptor (Fig. S3). To verify this antiregenerative effect of androgens on cTECs during the recovery of thymopoietic function, female mice were virilized by treatment with 5 $\alpha$ -dihydrotestosterone (5 $\alpha$ -DHT); as expected, this intervention essentially abolished thymopoietic recovery (Fig. 4D). Of note, T-cell numbers in males castrated after DT treatment (Fig. 4C) exceeded those observed in female mice after DT treatment (Fig. 4A) ( $P < 0.05$ ), providing evidence that the intrinsic mechanism of regeneration and the effects of gonadectomy independently affect the cTEC compartment.

## Discussion

Here, we describe a unique tissue-specific genetic system for cortical thymic epithelial cells. Our conditional model for cell-type-specific cytotoxicity provides direct evidence for the notion that the cTEC compartment is required for early stages of T-cell development (10, 11, 15) and that the number of cTECs influences the magnitude of T-cell production in the thymus. cTECs express *Ccl25* and *Cxcl12* chemokines and the Notch ligand *Dll4* (15), thus providing essential cues for the attraction (19) and specification (20, 21) of lymphocyte progenitors. Proliferation of early thymocytes is supported by the local production of IL-7 and Scf cytokines, whereas their positive selection is regulated by MHC expression. All of these environmental features are lost with the acute collapse of the cTEC compartment. The demise of immature thymocytes is correspondingly rapid, suggesting that sustained exposure to stromal support structures is vital for their survival. In addition, our results demonstrate that, after acute loss, cTECs possess the capacity to proliferate vigorously, albeit in a sexually dimorphic manner. Whether this compensatory growth is the result of increased proliferation of cTEC progenitors or of differentiated cTECs (or both) remains to be clarified. It is unclear why this latent regenerative potential of cTECs is not activated during the age-related physiological involution of the thymus, which affects males and females alike. These results suggest a multilayered regulation of the number of cTECs. In normal mice, the regenerative program of the epithelial compartment is maintained in an inactive state and thus fails to counter the progressive decline of the cTEC compartment

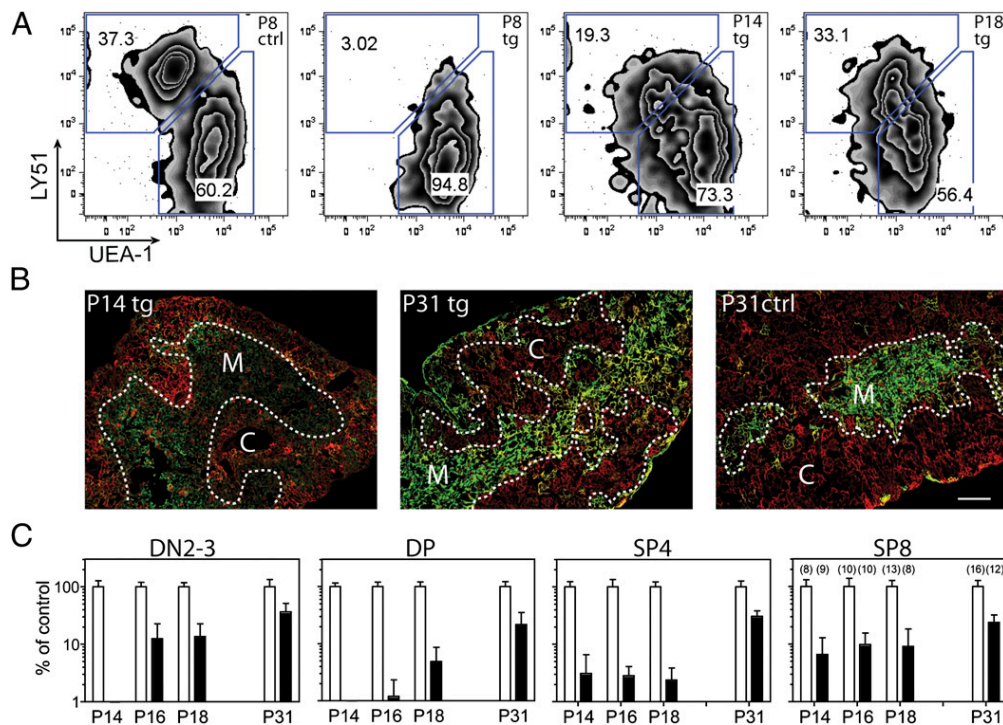


**Fig. 3.** Regenerative capacity of cTECs after near-total ablation in young mice. (A) Phenotypic characterization of TECs ( $CD45^-Epcam^+$ ) at various time points after DT treatment at P7; the presence of cTECs and mTECs was determined by flow cytometry. (B) Representative cryosections of thymic tissue at various time points after DT treatment at P7 stained with antibodies for an mTEC marker (cytokeratin 5, green fluorescence) and a cTEC marker (cytokeratin 8, red fluorescence). (Scale bar, 100  $\mu$ m.) (C) Temporal changes in thymocyte subsets after DT treatment. DN2-3 ( $Lin^-CD25^+$ ); DP thymocytes ( $CD4^+CD8^+$ );  $CD4^+$  single positive;  $CD8^+$  single positive; cell numbers are expressed relative to age-matched control mice (mean  $\pm$  SD) (for absolute numbers see [Dataset S1](#)); the number of animals in each group is given in parentheses Above bars.

during aging. However, this inhibition is lessened in the event of acute cTEC loss, providing direct evidence for the latent state of regenerative capacity. Sex hormones provide an additional, but independent, means of controlling regeneration: androgens suppress this process, providing an explanation as to why regeneration occurs only in adult females. At present, we can only speculate about the mechanism(s) that is responsible for maintaining the cTEC compartment in a latent state with respect to regeneration. One possibility is that immature thymocytes suppress the proliferation of cTECs; the loss of immature thymocytes (resulting from the compromising cTEC compartment) may mimic a fetal thymus, where the ratio of thymocytes to cTECs is much lower, and cTECs might be capable of resuming their proliferative state. Alternatively, it is possible that, under physiological conditions, proliferation of cTECs is negatively controlled by direct cTEC-cTEC interactions. Indeed, at the tissue level, the main difference between involution and cTEC ablation is that in the latter, cell-cell contact between cTECs is lost. This implies that cTEC-specific adhesion molecules (22) are attractive pharmacological targets to improve thymic function in adults.

## Methods

**Mice.** C57BL/6 ( $CD45.2^+$ ) mice and congenic C57BL/6 ( $CD45.1^+$ ) mice were bred in and provided by the animal facility of the Max Planck Institute of Immunobiology and Epigenetics, Freiburg, Germany. The *Ccx-Ckr1:eGFP* mouse strain has been described (7). *Ccx-Ckr1:hdTR* mice were generated using a genomic BAC clone (BAC RP23-362K3, obtained from the BACPAC Resources Center at the Children's Hospital Oakland Research Institute, Oakland, California) that was modified by homologous recombination using the Red/ET kit (Gene Bridges) as follows: The human heparin-binding EGF-like growth factor cDNA (HBEGF, also known as hDTR; GenBank accession no. NM\_001945) was recombined into the single coding exon of *Ccx-Ckr1* (compare to GenBank accession no. NM\_145700). The modified BAC DNA

was injected in circular form into pronuclei of FVB mice according to standard protocols. Cell ablation was achieved by a single i.p. injection of DT (30 ng/g body mass) (List Biological Laboratories) unless stated otherwise. Note that, after birth, mice heterozygous or homozygous for the *Ccx-Ckr1-eGFP* knock-in allele have no overt thymus phenotype (7).

**Thymic Stromal Cell Isolation by Collagenase/Dispase Digestion.** Thymic lobes were trimmed of fat and connective tissue, then finely minced with scissors, and the resulting fragments were mechanically dissociated in RPMI-1640 (PAA) containing 2% FCS (PAN Biotech) to release the majority of thymocytes. Fragments were allowed to settle on ice and the supernatant (containing thymocytes) was discarded. The supernatant was replaced with fresh medium until the supernatant became clear (typically three to five changes). The thymic stromal tissue fragments were then incubated in 1 mL of digestion medium (prepared by mixing 800  $\mu$ L RPMI 1640-2% FCS (vol/vol), 100  $\mu$ L collagenase type 4 (2 mg/mL; Worthington), 100  $\mu$ L dispase (2 mg/mL; Worthington), 0.5  $\mu$ L DNaseI (5 mg/mL; MP Biomedicals) for 30 min at 37  $^{\circ}$ C in an Eppendorf thermomixer. After this incubation step, samples were mechanically dissociated, undigested tissue fragments were allowed to settle, and the supernatant was removed and stored on ice. The remaining thymic fragments were subjected to a second digestion in fresh digestion medium. After the second digestion, samples were mechanically dissociated and 500  $\mu$ L of stop solution [485  $\mu$ L RPMI-1640 2% FCS + 15  $\mu$ L EDTA (500 mM)] were added to each sample. After a 5-min incubation at 37  $^{\circ}$ C, the two samples were combined and the cells washed with 10 mL MACS buffer (PBS-5 mM EDTA-0.3% BSA).

**Immunohistochemistry Analysis.** Thymi were fixed with 4% paraformaldehyde for 60-120 min at 4  $^{\circ}$ C and washed in PBS (without  $Mg^{2+}$  and  $Ca^{2+}$ ), followed by an overnight incubation in PBS (without  $Mg^{2+}$  and  $Ca^{2+}$ ) containing 20% sucrose. Thymi were then embedded in OCT, frozen on dry ice, and subsequently cut using a Leica CM3050S cryostat (8  $\mu$ m thickness). After blocking with PBS containing 10% donkey serum (Jackson ImmunoResearch), sections were stained with primary and secondary antibodies diluted in PBS (without  $Mg^{2+}$  and  $Ca^{2+}$ )-0.5% BSA (wt/vol)-0.2% Tween-20 (vol/vol)-10% donkey serum (vol/vol). Sections were mounted with DAPI containing Fluoromount-G (SouthernBiotech) and visualized on a Zeiss Axio Imager Z1.

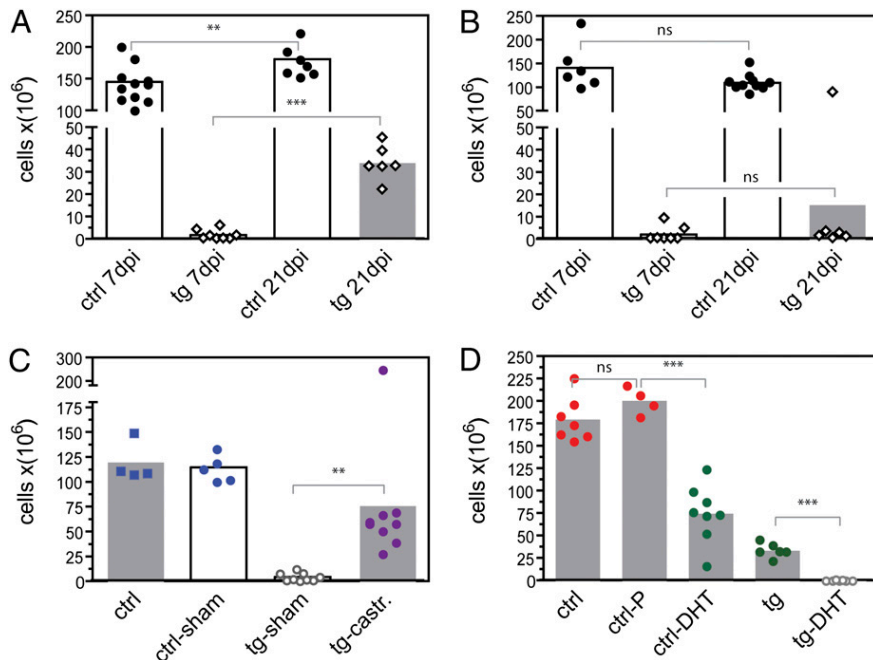


**Fig. 4.** Regenerative capacity of adult cTECs. (A and B) Recovery of DP thymocytes in adult female (A) and male (B) mice at various time points after DT treatment at 2–3 mo; dpi, days after toxin injection. Each dot represents one animal. (C) Castration of male mice 1 d after DT treatment improves DP recovery; sham, sham operation. (D) Virilization of female mice by 5 $\alpha$ -DHT prevents cTEC recovery; DT-treated adult female mice additionally received a slow-release pellet (p, placebo; DHT, 5 $\alpha$ -dihydroxytestosterone). For C and D, the absolute number of DP thymocytes was determined 3 wk after DT treatment (mean values; each symbol represents one animal). Statistical analysis was performed using Fisher's *t* test (\*\*\**P* < 0.001; \*\**P* < 0.01).

The primary antibodies directed against K8 (a kind gift of R. Kemler, Max Planck Institute of Immunobiology and Epigenetics, Freiburg, Germany), ERTR7 (Acris), and K5 (Covance) were detected using donkey- $\alpha$ -rat-Cy3 and donkey- $\alpha$ -rabbit-Cy5 (both from Jackson ImmunoResearch).

**Flow Cytometry and Sorting.** Flow cytometry analyses were performed on freshly prepared single-cell suspensions in MACS buffer [PBS (without Mg<sup>2+</sup> and Ca<sup>2+</sup>)-5 mM EDTA-0.3% (wt/vol) BSA].  $1 \times 10^6$  cells were blocked with MACS buffer additionally containing 10% (vol/vol) normal rat serum (Invitrogen) and stained using the following antibodies (clone designation in brackets): CD45.2 (B44), CD45.1 (A20), CD4 (GK1.5), CD4 (RM4.5), CD8a (53-6.7), CD3e (145-2C11), B220 (RA3-6B2), CD11c (HL3), CD11b (M1/70), TCRgd (GL3), TCRb (H57-597), NK1.1 (PK136), Gr1 (RB6-8C3), Ter119 (Ter-119), CD25 (PC61.5), CD44 (IM7), CD45 (30-F11), EpCAM (G8.8), CD31 (MEC13.3), Ly51 (6C3) (eBioscience, BD Pharmingen, BD Bioscience, or BioLegend); for staining with antibodies directed against the androgen receptor (clone 523339; R&D Systems), cells were treated with permeabilization buffer (eBioscience). The lineage mixture used for DN stainings contained antibodies directed against CD8a, CD3e, B220, CD11c, CD11b, TCRgd, TCRb, NK1.1, Gr1, and Ter119. Streptavidin (Sav) APC-eFluor780, SavPerCPCy5.5, Sav-APCCy7 (BD Pharmingen or eBioscience) and UEA-1-Bio (Vector) were also used to stain cells. Cell surface profiles were analyzed with a LSR II (BD Biosciences); cells were sorted using a MoFlo (Beckman Coulter) or Aria IIu (BD Biosciences).

**Surgical Castration.** Male mice received a single i.p. injection of DT (30 ng/g) 1 d before surgery. For surgical castration, mice were anesthetized and a small scrotal incision was made to reveal the testes. These were removed along with surrounding fatty tissue. The wound was closed using surgical suture. Sham castration was performed using the same surgical procedure, but without removal of the testes.

**Virilization of Female Mice.** Female mice received a single i.p. injection of DT (30 ng/g) 1 d before surgery. Mice were anesthetized for the implantation of 0.5-mg 21-d release 5 $\alpha$ -dihydrotestosterone or placebo pellets (Innovative Research). To implant the pellet, the skin on the lateral side of the neck of the animal was lifted. A small incision equal to the diameter of the pellet was made and forceps were used to make a small pocket for the pellet. Finally the pellet was placed inside this pocket and the incision was closed with surgical staples.

**Quantitative RT-PCR.** Cells sorted by flow cytometry were directly lysed in TRIzol reagent (Sigma). Total RNA was purified by chloroform extraction and precipitation with isopropanol. RNA samples were treated with RNase-free DNase (Roche) before first-strand cDNA synthesis primed with Oligo-dT using SuperScriptII (Invitrogen). The first-strand cDNA was used as a template in qPCR reactions after RNaseH digestion (Invitrogen). qRT-PCR was performed on a 7500 fast cyclor (Applied Biosystems) using Absolute Blue QPCR SYBR low Rox mix (Thermo Scientific) and results were analyzed according to the ddCT (difference of the differences of threshold cycle numbers) method. Primers were designed to span introns to avoid amplification of residual genomic DNA. The following primers were used: *Ccr-ckr1:eGFP*: TGAACCTGTGGC-CGTTTACGTC and CAAGATAAAGCGGGGTGA, amplicon size 193 bp; *Ccr-ckr1*: AGGTCCTCTGATTCTCTGC and GCAGGAAGACTTTTGCGAAC, amplicon size 195 bp, GenBank accession no. NM\_145700; *Ccr-ckr1:hDTR*: CAA-GATAAAGCGGGGTGA and GTCACCAGTGCCGAGAGAAC, amplicon size 187 bp; *Hprt*: TGTTGTTGGATATGCCCTTG and GGCCACAGGACTAGAACC, amplicon size 181 bp, GenBank accession no. NM\_013556.2.

**Bone Marrow Chimeras.** C57BL/6 (CD45.2 or Ly5.2) mice were lethally irradiated by two doses ( $\gamma$ -irradiation 4.5 Gy and 4 Gy) separated by a 3-h interval. Irradiated mice were maintained in individually ventilated cages with drinking water containing antibiotics [Trimethosol (5 mL/L); Selectavet]. Recipients received  $1 \times 10^7$  congenic (CD45.1/2 or Ly5.1/2) bone marrow cells (after lysis of red blood cells) by i.v. injection 24 h after the last irradiation. Mice were injected with DT (Sigma; 56  $\mu$ g/kg) intraperitoneally for 7 consecutive days before thymi were analyzed by flow cytometry 1 d after cessation of treatment.

**Thymus Transplantation.** Two thymic lobes of newborn *Ccr-ckr1:hDTR* mice were placed under the kidney capsule of one anesthetized syngeneic recipient mouse. Recipient mice were treated with DT (43  $\mu$ g/kg) for 3 consecutive days from day 41 after transplantation. Transplanted thymic lobes were isolated on day 4 after cessation of DT treatment and analyzed by flow cytometry.

**ACKNOWLEDGMENTS.** We thank C. Bleul and C. Benz for *Ccr-ckr1<sup>eGFP</sup>* mice, B. Kanzler for help with the generation of *Ccr-ckr1:hDTR* transgenic mice, C. Bleul for advice and helpful suggestions, B. Hammerschmidt for expert technical assistance, and the Max Planck Society for financial support.

1. Rudd BD, et al. (2011) Nonrandom attrition of the naive CD8<sup>+</sup> T-cell pool with aging governed by T-cell receptor:pMHC interactions. *Proc Natl Acad Sci USA* 108:13694–13699.
2. Lynch HE, et al. (2009) Thymic involution and immune reconstitution. *Trends Immunol* 30:366–373.
3. Holländer GA, Krenger W, Blazar BR (2010) Emerging strategies to boost thymic function. *Curr Opin Pharmacol* 10:443–453.
4. Taub DD, Murphy WJ, Longo DL (2010) Rejuvenation of the aging thymus: Growth hormone-mediated and ghrelin-mediated signaling pathways. *Curr Opin Pharmacol* 10:408–424.
5. Min H, Montecino-Rodriguez E, Dorshkind K (2006) Reassessing the role of growth hormone and sex steroids in thymic involution. *Clin Immunol* 118:117–123.
6. Griffith AV, Fallahi M, Venables T, Petrie HT (2012) Persistent degenerative changes in thymic organ function revealed by an inducible model of organ regrowth. *Aging Cell* 11:169–177.
7. Gray DHD, et al. (2006) Developmental kinetics, turnover, and stimulatory capacity of thymic epithelial cells. *Blood* 108:3777–3785.
8. Rossi SW, Jenkinson WE, Anderson G, Jenkinson EJ (2006) Clonal analysis reveals a common progenitor for thymic cortical and medullary epithelium. *Nature* 441:988–991.
9. Bleul CC, et al. (2006) Formation of a functional thymus initiated by a postnatal epithelial progenitor cell. *Nature* 441:992–996.
10. Anderson G, Lane PJL, Jenkinson EJ (2007) Generating intrathymic microenvironments to establish T-cell tolerance. *Nat Rev Immunol* 7:954–963.
11. Rodewald H-R (2008) Thymus organogenesis. *Annu Rev Immunol* 26:355–388.
12. Jenkinson WE, Bacon A, White AJ, Anderson G, Jenkinson EJ (2008) An epithelial progenitor pool regulates thymus growth. *J Immunol* 181:6101–6108.
13. Corbeaux T, et al. (2010) Thymopoiesis in mice depends on a *Foxn1*-positive thymic epithelial cell lineage. *Proc Natl Acad Sci USA* 107:16613–16618.
14. Rodewald HR, Paul S, Haller C, Bluethmann H, Blum C (2001) Thymus medulla consisting of epithelial islets each derived from a single progenitor. *Nature* 414:763–768.
15. Petrie HT, Zúñiga-Pflücker JC (2007) Zoned out: Functional mapping of stromal signaling microenvironments in the thymus. *Annu Rev Immunol* 25:649–679.
16. Heinzl K, Benz C, Bleul CC (2007) A silent chemokine receptor regulates steady-state leukocyte homing *in vivo*. *Proc Natl Acad Sci USA* 104:8421–8426.
17. Müller SM, et al. (2008) Neural crest origin of perivascular mesenchyme in the adult thymus. *J Immunol* 180:5344–5351.
18. Shakib S, et al. (2009) Checkpoints in the development of thymic cortical epithelial cells. *J Immunol* 182:130–137.
19. Calderón L, Boehm T (2011) Three chemokine receptors cooperatively regulate homing of hematopoietic progenitors to the embryonic mouse thymus. *Proc Natl Acad Sci USA* 108:7517–7522.
20. Hozumi K, et al. (2008) Delta-like 4 is indispensable in thymic environment specific for T cell development. *J Exp Med* 205:2507–2513.
21. Koch U, et al. (2008) Delta-like 4 is the essential, nonredundant ligand for Notch1 during thymic T cell lineage commitment. *J Exp Med* 205:2515–2523.
22. Perez-Moreno M, Jamora C, Fuchs E (2003) Sticky business: Orchestrating cellular signals at adherens junctions. *Cell* 112:535–548.